A SAMPLE RATE CONVERTER FOR MEASURING INSTRUMENTS OF POWER QUALITY INDICATORS

A. N. Serov, A. A. Shatokhin, N. A. Serov, G. V. Antipov

Abstract: Measurements of many power quality indicators are based on a spectrum measurement by means FFT. However, at a fixed sample rate and number of samples, the mains frequency deviation from nominal value causes distortions in the spectrum, often called spectrum leakage. To reduce spectrum leakage, sample rate is adjusted to the mains frequency. One of the adjustment methods uses a sample rate converter (SRC) and periodic measurements mains frequency that are required to control the SRC sample rate factor.

The report presents the results of a study of the SRC based on the Lagrange interpolator implemented on the Farrow structure. The results are obtained by analytical modeling and simulation.

Keywords: power quality indicators, sample rate convertor, Lagrange interpolator, Farrow structure.

1. Introduction

The power quality is quantitatively characterized by power quality indicators (PQI). To measure them, special power quality measuring instruments (PQMI) are used. Modern PQMI for measuring a number of PQI use, as a rule, the fast Fourier transform (FFT). Before the FFT is performed, M samples are accumulated on the measurement interval with duration T_N, where N is the number of the main component periods ($N = 10$ for 50 Hz power supply systems). The most efficient FFT algorithms require that M be equal of degree two or four.

However, at a fixed sample rate f_s and M, the deviation of the mains frequency f_1 from rated value causes the distortions of spectrum, often called by spectrum leakage: the initial spectrum changes and additional components appear.

To reduce the spectrum leakage, the following basic methods are used: weighting functions; phase-locked loop (PLL); resampling.

Although weighting functions allow reducing additional components in the spectrum, distortions of the original components of the spectrum can be aggravated. Therefore, this method is not suitable for accurate measurement of the voltage or current spectrum.

In the case of PLL, the generator starts the ADC with a sample rate f_s, which tracks changes in f_1. The main drawback of this method is the dependence of the PQMI digital filters frequency responses on the sample rate f_s.

In the case of resampling, the signals are sampled at a constant sample rate f_{s1}. Due to this, the digital filters frequency responses remain constant when the mains frequency f_1 is varied. To reduce the spectrum leakage, the samples are processed by a sample rate converter (SRC), whose algorithm is usually implemented programmatically.

According to [1], it is required to adjust the sample rate f_{s2} with an error of not more than 0.03 %. This error can only be provided by the SRC with an arbitrary value of the sample rate conversion factor (ASRC – arbitrary sample rate converter). In this ASRC, the fractional part of the conversion factor can take any value.

The report describes the operation principle, structure, error, and simulation of the ASRC.

2. The operation principle of the arbitrary sample rate converter

The algorithm of the ASRC should calculate the values of the signal samples at new instants, located between the original samples, as shown in Fig. 1. Here, n and m are the sample indices, respectively, at the input and output of the ASRC (indexing starts from zero); $x(t)$ is an analog signal whose discrete samples are transmitted to the input of the ASRC with a step T_{s1}. At the output of the ASRC, it is necessary to obtain a sequence of samples y[I] with step T_{s2}, which are approximations of $x(t_m)$.

The current sample $y[m]$ is calculated using an interpolation polynomial of order L. To do this, a set of $(L+1)$ original samples (two in Fig. 1) is used and μ_m is the position between the samples, i.e. the fraction of the original sampling step T_{s1}. The last sample in this set has the index n_m, relative to which the previous L samples of the set are determined. The value μ_m is calculated from the conditional zero value located in the central interval of input samples (dotted line between n_{m-1} and n_m in Fig. 1). The subscript "m"

emphasizes that the corresponding value is a function of the ASRC output sample index.

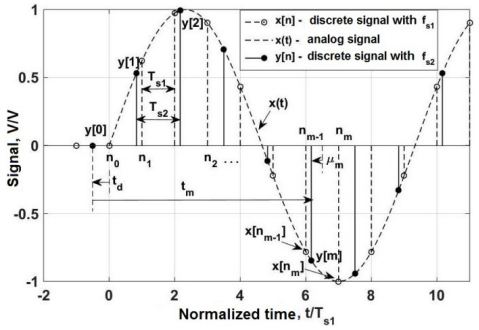

Fig. 1. Time relations between the original and the output samples of the ASRC

Thus, the main operation of the ASRC is an resampling, i.e. determination of the analog signal values in arbitrary positions between the original samples. Resampling is usually based on Lagrange interpolation. It is also known that interpolation in the form of Stirling is used in PQMI [2]. On the other hand, each output ASRC sample can be interpreted as an input delay equal to a part of T_{s1}. However, the delay should change during the operation of the ASRC and preferably with a single control parameter.

In the most general form, resampling is described by a finite convolution [3, 4]. In [5], a unified convolution notation was proposed, based on the system of counting nodes of base points relative to the zero point of value μ_m, as shown in Fig. 2. Here the base point is the pair: time and the corresponding input sample. A node is the abscissa of the base point, i.e. value of time. The positive direction of value μ_m coincides with the time axis. The nodes of the base points of the resampling algorithm form a decreasing arithmetic progression with a minus 1 common difference, since the nodes are normalized to the input sampling step T_{s1}.

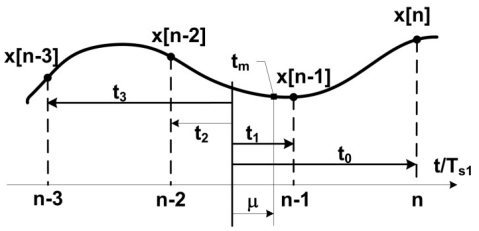

Fig. 2. The system of counting the nodes of the base points (for the variables μ and n, the index m is omitted)

Using the notation of the base point sets, the discrete convolution is defined with an index range from 0 to L [5]:

$$y(t_m) = y[m] = \sum_{l=0}^{L} x[n_m - l]h_l(\mu_m), \quad (1)$$

To reduce the resampling error and the number of calculations, the zero reference point of the nodes and the position between the samples μ_m are selected in the middle of the node range of base points whose samples are included in the convolution (1) [3 - 6]. In this case, symmetrical nodes of base points and a symmetrical range of μ_m values are formed:

$$t_l = \frac{L}{2} - l; \;\; t_{L-l} = -t_l \;\; для \; 0 \le l \le L, \quad (2)$$

$$-0{,}5 \le \mu_m < 0{,}5 \quad . \quad (3)$$

Symmetric nodes ensure the symmetry of the coefficients h_l (μ_m) when computing the discrete filter (1), which leads to more efficient algorithms.

According to the principle of the ASRC operation, the identity is valid (see Fig. 1):

$$\left(n_m - \frac{L}{2} + \mu_m\right) T_{s1} = mT_{s2} - t_d \quad (4)$$

where t_d is the delay of the ASRC output sample y[m] relative to the ASRC input sample $x[n_m]$ (the positive direction of t_d is opposite to the time axis).

In order to give causality to the ASRC algorithm (real-time capabilities), the minimum value of t_d should be (T_{s1} L)/2. Then the identity (4) takes the form:

$$\left(n_m - \frac{L}{2} + \mu_m\right) T_{s1} = mT_{s2} - T_{s1}\frac{L}{2}. \quad (5)$$

The sample index n_m and the position between the samples μ_m are calculated from (5):

$$\mu_m = \frac{mf_{s1}}{f_{s2}} - n_m, \quad (6)$$

$$n_m = round\left(\frac{mf_{s1}}{f_{s2}}\right) \quad (7)$$

where round (·) – rounding to the nearest integer.

3. Implementation of interpolation.

The Farrow structure

Lagrange's interpolation is effectively implemented by the structure proposed by Farrow

[7]. The Farrow structure (the Farrow filter) is an FIR filter with the coefficients $h_l(\mu_m)$ that can be changed by the variable μ_m. The scheme of the generalized Farrow structure is shown in Fig. 3. Here, $H_l(z)$ denotes the transfer function of one of the M+1 FIR filters of order L, which are called subfilters of the Farrow structure. The outputs of the subfilters form the coefficients of the polynomial of μ_m of degree M. The embedded calculations of the polynomial are performed according to the Horner scheme. In the general case, M and L are independent. In the particular case when the interpolation condition is satisfied, M=L.

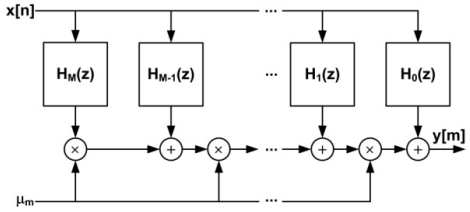

Fig. 3. The Farrow structure diagram

Algorithm for discrete filtering of the Farrow structure for Lagrange interpolation in matrix form is the following:

$$y[\mathrm{m}] = \mathbf{M}\times\mathbf{C}\times\mathbf{X} \qquad (8)$$

where the matrices: $\mathbf{M} = [\mu^0 \quad \ldots \quad \mu^L]$;

$$\mathbf{C} = \begin{bmatrix} c_{00} & \cdots & c_{0L} \\ \cdots & \cdots & \cdots \\ c_{L0} & \cdots & c_{LL} \end{bmatrix} = \mathbf{V^{-1}}; \mathbf{X} = \begin{bmatrix} x[n] \\ \cdots \\ x[n-L] \end{bmatrix};$$

V^{-1} is the inverse Vandermonde matrix.

The Vandermonde matrix is a square matrix whose columns are the element-by-element powers of the base points nodes t_l, starting at the zero power, where t_l is defined by (2). To simplify the notation, the subscript "m" of the variables μ and n is omitted.

The rows of the matrix C are the coefficients of the subfilters of the Farrow structure, starting with the subfilter whose output determines the coefficient of the polynomial with zero power μ_m. The first coefficient in the rows corresponds to the current sample $x[n_m]$.

The matrix form of the filtration equation (8) is useful for simulation in an interactive MATLAB environment. In PQMI, it is advisable to use a modified Farrow structure to reduce calculations, where the number of multiplications is approximately halved due to the symmetry of the coefficients in the subfilters $H_k(z)$. In addition, the number of arithmetic operations can be reduced due to the zero and unit coefficient of the subfilters. The second order interpolator shown in Fig. 4, requires 9 arithmetic operations instead of 19 when implemented on the classical Farrow structure.

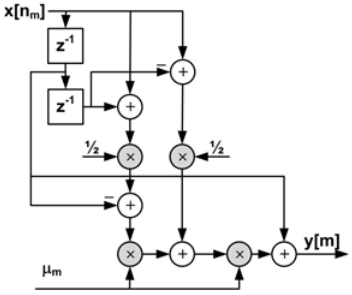

Fig. 4. Modified Farrow structure for Lagrange interpolator of the second order

4. ASRC Structure

As noted earlier, to reduce the spectrum measurement error, sampling frequency should be adjusted to the f_1. This problem is solved by ASRC, the structural diagram of which is shown in Fig. 5 with details of interpolator control.

The input samples $x[n]$ arrive at a constant sample rate f_{s1}. The output samples $y[m]$ correspond to the sample rate f_{s2}, the value of which is maintained directly proportional to the value f_{s1}. For this purpose, the meter f_1 periodically supplies the result of its measurement $\widetilde{f_1}$ to the ASRC controller, where f_{s2} is calculated by the formula:

$$f_{s2} = \frac{\widetilde{f_1}}{f_{1,nom}} f_{s2,nom} \qquad (9)$$

where $f_{1,nom}$ = 50 Hz; $f_{s2,nom}$ is the output sample rate of the ASRC at f_1=$f_{1,nom}$.

The calculation of $y[m]$ requires the calculation of μ_m and n_m, respectively, using formulas (6) and (7).

As noted in [2], the practical ASRC control algorithm should use increments of counter variables rather than their absolute values to prevent overflow handling. Subtract n_{m-1} from the left and right sides (7):

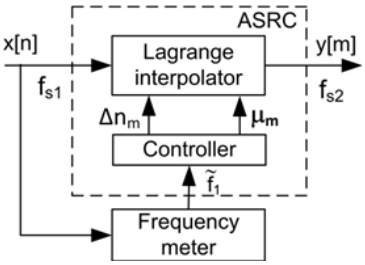

Fig. 5. ASRC structural diagram

$$\Delta n_m = n_m - n_{m-1} = round\left(m\frac{f_{s1}}{f_{s2}}\right) - n_{m-1}.$$

Since n_{m-1} is an integer and does not exceed n_m, it can be entered under the sign of the operation $round(\cdot)$. Then the last expression takes the form:

$$\Delta n_m = round\left(m\frac{f_{s1}}{f_{s2}} - n_{m-1}\right) \qquad (10)$$

where Δn_m is the number of samples to be updated in the input buffer (delay buffer) of the Farrow structure to calculate the next sample at the ASRC output.

Using (6), we write μ_{m-1} as

$$\mu_{m-1} = (m-1)\frac{f_{s1}}{f_{s2}} - n_{m-1}. \qquad (11)$$

Whence we find the expression for n_{m-1} and substitute it into the formula (10). As a result, we finally get

$$\Delta n_m = round\left(\frac{f_{s1}}{f_{s2}} + \mu_{m-1}\right). \qquad (12)$$

The recursive formula for μ_m is obtained by replacing the first term on the right-hand side of (6) with its expression from (11):

$$\mu_m = \mu_{m-1} + \frac{f_{s1}}{f_{s2}} - \Delta n_m. \qquad (13)$$

5. Analysis of the measurement error spectrum due to the imperfection of the ASRC

The spectrum measurement error consists of the error in measuring the frequency f_1 and the error of the ASRC interpolator. The first component is considered in [8]. Here we consider the error of the ASRC interpolator and the corresponding error of the spectrum measurement.

The frequency response of the ideal interpolator $\dot{H}_{ref}(\omega, \mu_m)$ has the form:

$$\dot{H}_{ref}(\omega, \mu_m) = e^{j\varphi_{ref}} \qquad (14)$$

where $\omega = 2\pi f/f_{s1}$ is the angular frequency normalized to the frequency f_{s1}.

The ideal interpolator can be interpreted as an ideal delay with linear phase response: $\varphi_{ref} = \omega(\mu_m - L/2)$ and single amplitude-frequency response: $|\dot{H}_{ref}| = 1$. The term $L/2$ in the phase response is due to the choice of the zero reference point μ_m in the middle of the range of base points nodes.

The interpolator frequency response can be represented as follows:

$$\dot{H}(\omega, \mu_m) = (1 + \Delta H)e^{j(\varphi_{ref} + \Delta\varphi)} \qquad (15)$$

where $\Delta\varphi = arg\,\dot{H}(\omega, \mu_m) - \varphi_{ref}$; $\Delta H = |\dot{H}(\omega, \mu_m)| - 1$; ΔH and $\Delta\varphi$ are functions of ω and μ_m.

Suppose that a sinusoidal discrete signal with a unit amplitude is fed to the interpolator input: $x[n_m] = sin\omega n_m$. Then, taking into account (14) and (15), the absolute error at the output of the interpolator in the steady state $\Delta y[m]$ is:

$$\Delta y[m] = (1 + \Delta H)\sin(\omega n_m + \varphi_{ref} + \Delta\varphi) - \\ - \sin(\omega n_m + \varphi_{ref}) \qquad (16)$$

We simplify expression (16): we decompose the first sine into a Taylor series in the neighborhood of the argument $(\omega n_m + \varphi_{ref})$, limited to two terms. As a result, we get

$$\Delta y[m] = \sqrt{\Delta H^2 + \Delta\varphi^2}\sin\theta \qquad (17)$$

where $\theta = \omega n_m + \varphi_{ref} + arctg\frac{\Delta\varphi}{\Delta H}$.

It follows from the formula (17) that the interpolator error and, consequently, the ASRC is determined by the error of both the interpolator amplitude-frequency response and phase response.

In the matrix form, the interpolator frequency response has the form:

$$\dot{H}(\omega, \mu_m) = \mathbf{M} \times \mathbf{C} \times \boldsymbol{W}, \qquad (18)$$

where the matrix $\boldsymbol{W^T} = \left[1\ e^{-j\omega}\ \ldots\ e^{-j\omega L}\right]$.

To obtain a more convenient analytical form of ΔH and $\Delta\varphi$, their approximations are found in the form of polynomials of two variables: ω and μ_m (Table 1). The approximations are obtained by expanding in a Taylor series of the modulus and phase of the frequency response (18).

Table 1. Some approximations of ΔH and Δφ for 0 – 3 order interpolators

L	ΔH	Δφ
0	0	$-\omega\mu_m$
1	$\frac{\omega^2}{2}\left(\mu_m^2-\frac{1}{4}\right)$	$-\frac{\omega^3}{3}\mu_m\left(\mu_m^2-\frac{1}{4}\right)$
2	$\frac{\omega^4}{8}\mu_m^2(\mu_m^2-1)$	$\frac{\omega^3}{6}\mu_m(\mu_m^2-1)$
3	$\frac{19\omega^4}{200}\left(\mu_m^2-\frac{1}{4}\right)$	$-\frac{19\omega^5}{250}\mu_m\left(\mu_m^2-\frac{1}{4}\right)$

According to Table 1, the following conclusions can be drawn:

1. Increasing f_{s1} (decreasing ω) and/or the interpolator order leads to a significant decrease in the interpolator error. However, this puts high demands on the processor speed.

2. For the main component (f_1 = 50 Hz), the interpolator error is insignificant, since in this case $\omega<<1$. Therefore, the sample rate f_{s1} and the interpolator order must be selected based on the measurement error of the higher harmonics.

The expressions presented in Table 1 allow, for a given frequency f_{s1}, to estimate from above the interpolator error and, consequently, the error in measuring the spectrum.

A more accurate analytical modeling of the spectrum error, suitable for analysis, requires an explicit expression for μ_m as a function of the index m. However, it is not possible to obtain such an expression. Therefore, to analyze the spectrum measurement error due to the non-ideal interpolator, a special technique based on the ASRC simulation was developed.

Figure 6 shows the maximum in modulus relative errors in measuring of the amplitude spectrum δ_{max} obtained by simulation and corresponding to them permissible errors δ_{lim} according to GOST R 51317.4.7-2008: 5% for $K_h \geq 1$ % and $(5/K_h)$ % for 1 %>K_h≥0.2 %, where K_h is the voltage harmonic coefficient with the index h. Figure 7 shows the maximum in modulus absolute errors of phase measurement Δ_max obtained by simulation and the corresponding to them permissible errors Δ_{lim} according to GOST R 8.655-2009: 1° for $K_h \geq 5$ %; 5° for 5 %>K_h≥1 %; 10° for 1 %>K_h≥0.2 %. For the main component: δ_max=0.021 % (δ_{lim}=0.1 %) and Δ_{max}=0.0052° (Δ_{lim}=0.2°). The input signal is polyharmonic, the harmonic amplitudes are chosen equal to one and a half limit values according to GOST 32144-2013. The variation range of the fundamental frequency f_1 was set to ±15% in increments of 0.01%.

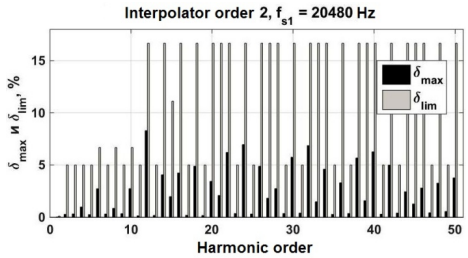

Fig. 6. Maximum and permissible errors of the amplitude spectrum

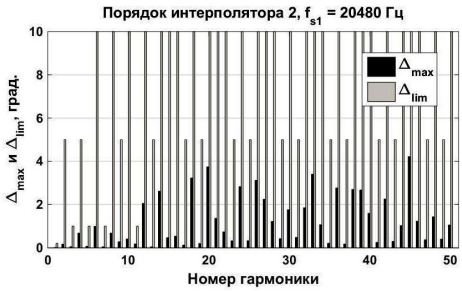

Fig. 7. Maximum and permissible errors of the phase spectrum

The corresponding averaged spectra calculated using 15 successive FFT on the T_N interval were taken as the measurement results of the amplitude and phase spectra. The spectrum measurement error was calculated for each f_1 value. The error δ_{max} and $\Delta_{\max}$ was determined for each harmonic as the maximum modulo value over the entire f_1 variation range.

It can be seen from figures 6 and 7 that the Lagrange interpolator of the second order at sample rate f_{s1} equal to 20480 Hz ensures the accuracy of the spectrum measurement with a sufficient margin.

6. Conclusion

Based on the above material, we can draw the following conclusions:

1. The formulas presented in table 1 allow us to estimate the spectrum measurement error due to the interpolator imperfection at the designing stage of the PQMI.

2. The interpolator implementation on the modified Farrow structure allows reducing the number of calculations.

3. It was established by simulation that a second-

order Lagrange interpolator with a sample rate at the input of 20480 Hz ensures the spectrum measurement accuracy with a sufficient margin.

7. References

[1] GOST R 51317.4.7 (IEC 6100-4-7:2002).

[2] **S.N. Mikhalin, V.M. Gevorkyan.** Problemy tsifrovoy obrabotki signalov v sisteme avtomatizirovannogo kontrolya kachestva i ucheta kolichestva elektroenergii (ASKUE) // Vestnik MEI. - 2005. - № 1. - S. 86-92.

[3] **F.M. Gardner.** *Interpolation in digital modems – Part I: Fundamentals.* IEEE Transactions on Communications, vol. 41, no. 3, pp. 502-508, Mar. 1993.

[4] **L. Erup, F. M. Gardner, and R. A. Harris.** *Interpolation in digital modems – Part II: Implementation and performance.* IEEE Transactions on Communications, vol. 41, no. 6, pp. 998-1006, June 1993.

[5] **Andreas Franck.** *Efficient Algorithms for Arbitrary Sample Rate Conversion with Application to Wave Field Synthesis: PhD thesis*/Technische Universität Ilmenau. Ilmenau, 2012. 269 pp.

[6] **T. I. Laakso, V. Vlilimiiki, M. Karjalainen, and U. K. Laine.** *Splitting the unit delay: Tools for fractional delay filter design.* IEEE Signal Processing Mag., vol. 13, pp. 30-60, Jan. 1996.

[7] **C. W. Farrow.** *A continuously variable digital delay element.* IEEE International Symposium on Circuits and Systems, Espoo, Finland, vol. 3, pp. 2641-2645, June 1988.

[8] **Andrey Serov, Alexander Shatokhin, Ivan Konchalovsky.** *Research of influence of mains frequency deviation on voltage spectrum measurement error by DFT method.* Proceedings of the 27th International Scientific Symposium «Metrology and Metrology Assurance 2017». – Sozopol, Bulgaria, 2017, ISSN: 1313-9126, pp. 185–189.

Information about the Authors:

Serov Andrey Nikolaevich, NRU «MPEI» – Computer systems and networks (2006). Ph.D. (2017), assistant professor (2018). Measurement of high currents and power. NRU «MPEI», AVTI, Department IIT.

Web: *mpei.ru*

e-mail: serov.an.iit@yandex.ru

Shatokhin Alexander Alekseevich, NRU «MPEI» – Information and measuring technique (1973). Ph.D. (1985), assistant professor (1986). Digital signal processing. NRU «MPEI», AVTI, Department IIT.

Web: *mpei.ru*

e-mail: sh1@yandex.ru

Serov Nikolai Andreevich, NRU «MPEI» – Information and measuring technique (1971). Ph.D. (1985), assistant professor (1986). Analog measuring devices. NRU «MPEI», AVTI, Department IIT.

Web: *mpei.ru*

e-mail: serna2004@list.ru

Antipov Gennady Viktorovich, NRU «MPEI» – Information and measuring technique (1978). Ph.D. (1991), assistant professor (1993). Digital signal processing. NRU «MPEI», AVTI, Department IIT.

Web: *mpei.ru*

e-mail: antipovgv@mpei.ru